Separation of Fischer–Tropsch Wax from Catalyst Using Near-Critical Fluid Extraction: Analysis of Process Feasibility

ARTICLE *in* ENERGY & FUELS · APRIL 1999

Impact Factor: 2.79 · DOI: 10.1021/ef980208u

4 AUTHORS, INCLUDING:

Peter K Kilpatrick

97 PUBLICATIONS **2,643** CITATIONS

SEE PROFILE

Separation of Fischer−Tropsch Wax from Catalyst Using Near-Critical Fluid Extraction: Analysis of Process Feasibility

Joan M. Biales,† Ying Di Wan,‡ Peter K. Kilpatrick, and George W. Roberts*

Department of Chemical Engineering, Box 7905, North Carolina State University, Raleigh, North Carolina 27695-7905

Received September 30, 1998

The technical feasibility of a near-critical fluid extraction (NCE) process for the recovery of heavy normal paraffins from a Fischer−Tropsch slurry reactor has been analyzed. Process simulations were carried out using the ASPEN PLUS program, considering 100 individual compounds from C_1 to C_{100}. Four light solvents were evaluated: *n*-pentane, *n*-hexane, *n*-heptane, and *n*-octane. These four compounds are major products of the F−T reaction. Most of the analysis was concentrated in two regions: (1) high solvent/product ratios (ca. 20/1), such that product could be recovered by temperature-retrograde condensation; and, (2) low solvent/product ratios (ca. 3/1). The latter region appeared to require higher extraction temperatures and higher slurry flowrates, but had several attractive features such as lower vapor flowrates, lower solvent makeup rates, and lower energy requirements. The concentration of solvent in the product from the NCE process was never low enough for the process to be self-sufficient in solvent, when the flowsheet contained only one product recovery unit. Self-sufficiency was obtained with multiple recovery units. The NCE process appears to be feasible, and has many attractive features. However, the existing thermodynamic database is not sufficient to support an optimum process design.

Introduction

Approximately 17 million barrels/day of petroleum are consumed in the United States, of which almost half is imported,[1] and there are similar deficiencies of liquid fuels in other parts of the world. At the same time, extensive reserves of coal and natural gas exist in many geographical regions that lack sufficient petroleum. Therefore, there is a significant international incentive to convert readily available solid and gaseous fuels into liquids. The Fischer−Tropsch (F−T) process is one way to carry out this conversion.

In the F−T synthesis, carbon oxides are reacted with hydrogen to form higher hydrocarbons and oxygenates.[2] The product is a complex mixture of paraffins, olefins, and alcohols of different carbon numbers. The exact composition depends on the particular catalyst and operating conditions that are employed, but normal paraffins are a dominant component of most product streams. A mixture of hydrogen and carbon oxides, known as "synthesis gas" or "syngas", can be produced from materials such as coal, natural gas, waste biomass, and petroleum coke. A great deal of recent F−T development has been concentrated on converting so-called "remote" natural gas into a synthetic crude oil that is compatible with the existing refining infrastructure.

A generalized F−T reaction for the formation of high-carbon-number paraffins is:

$$n\mathrm{CO} + 2n\mathrm{H_2} \rightarrow (\mathrm{CH_2})_n + n\mathrm{H_2O} \qquad \text{(A)}$$

$$\Delta H_R\ (298\ \mathrm{K}) \cong -40\ \mathrm{kcal/mol\ CO}$$

The reaction is highly exothermic, which creates a major challenge in the design of the F−T reactor. Several types of F−T reactors are used commercially including fixed-bed, fluidized-bed, and circulating-fluidized-bed reactors.[3] However, slurry bubble column (SBC) reactors have been the focus of recent development because their near-isothermal operation makes them ideal for exothermic reactions. The earliest studies of F−T synthesis in a SBC reactor were carried out in Germany between 1938 and 1953.[4] Other early studies using slurry reactors took place in the United States[5] and the United Kingdom.[6] A 2500 bbl/day pilot plant based on a SBC reactor has been operated in South Africa.[3] The Federal Energy Technology Center's Alternative Fuels Development Unit (AFDU) in La Porte, TX,

* Author to whom correspondence should be addressed. Fax: (919)-515-3465. E-mail: groberts@eos.ncsu.edu.

† Current address: E. I. du Pont de Nemours & Co., Chattanooga, TN 37415.

‡ Current address: Procter & Gamble Company, Brown Summit, NC 27214.

(1) *Energy Statistics Sourcebook, 10th ed.*; Leung, R., Ed.; Penn Well Publishing Company: Tulsa, OK, 1995; p 338.

(2) Fischer, F.; Tropsch, H. Process for the Production of Paraffin-Hydrocarbons With More Than One Carbon Atom. U.S. Patent 1,746,-464, February 11, 1930.

(3) Jager, B. *Sasol's Advanced Commercial Fischer−Tropsch Processes*; American Institute of Chemical Engineers 1997 Spring National Meeting, March 9−13, 1997, Houston, TX; Paper 27c.

(4) Kölbel, H.; Ralek, M. *Catal. Rev.−Sci. Eng.* **1980**, *21*, 225−274.

(5) Schlesinger, M. D.; Crowell, J. H.; Leva, M.; Storch, H. H. *Ind. Eng. Chem. Process Dev.* **1951**, *43*, 1474−1479.

(6) Farley, R.; Ray, D. J. *J. Inst. Pet.* **1964**, *50*, 27−46.

10.1021/ef980208u CCC: $18.00
Published on Web 04/17/1999

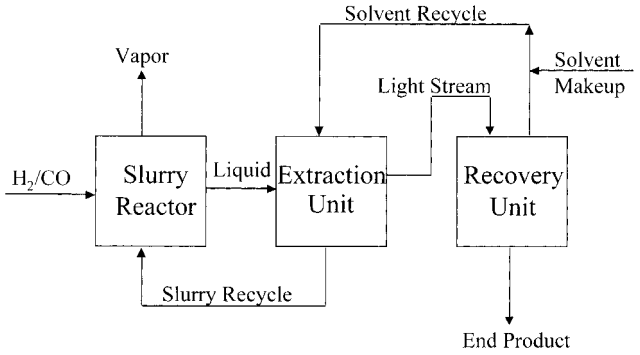

Figure 1. Schematic diagram of near-critical extraction process for separating Fischer−Tropsch wax from catalyst.

is being used to study SBC F−T reactors,[7] and SBC reactors are planned for several commercial processes.[3,8]

The major obstacle to using SBC reactors for the F−T synthesis is separating the product from the catalyst slurry. Low-molecular-weight reaction products such as methane leave the reactor as vapor. However, high-molecular-weight products remain in the liquid phase. This requires that small catalyst particles with diameters in the range of 0.1 to 100 μm be separated from a viscous liquid product. The separated liquid must be essentially free of catalyst particles so that it can be processed in conventional refinery operations. As discussed below, the liquid may contain paraffins with carbon numbers up to about 100. These compounds make the liquid waxy in nature and the heavy liquid product sometimes is referred to as "wax".

Many techniques have been studied for separating a F−T catalyst from the waxy product,[9] including sedimentation by gravity or centrifugal force, internal and external filters, and magnetic separation. Historically, filtration has received the most attention but it has been plagued with operational problems such as filter plugging, which has caused significant downtime and raised serious questions concerning the technical feasibility of filtration as a catalyst/wax separation technique.

More recently, a near-critical fluid extraction (NCE) process has been described for the separation of F−T catalyst and wax.[10] This process, shown schematically in Figure 1, involves continuously removing a catalyst/wax slurry from the SBC reactor and contacting it in the extraction unit with a light hydrocarbon solvent near its critical point. In the near-critical region, the solvent has liquidlike densities[11] and the solubility of the heavy hydrocarbons can be "tuned" by varying the temperature and/or pressure. Some of the heavy liquid in the slurry is extracted into the light phase, and some of the light solvent dissolves into the slurry. The light and heavy phases are separated, and the slurry is recycled to the reactor. The light phase passes to a recovery unit, which operates at a different pressure and/or temperature than the extraction unit. As a result, some of the heavier components in the feed condense to form a second, heavy phase which constitutes the end product stream. The remaining light phase is recyled to the extraction unit. A solvent makeup stream of the light solvent is added to this recycle stream to compensate for solvent that is lost in the final product and in the vapor stream leaving the reactor.

Supercritical and near-critical extraction processes have been used in a number of industrial applications, including the residuum oil supercritical extraction (ROSE) process for deasphalting vacuum-reduced crudes.[12] Super- and near-critical extraction have also been applied successfully to problems involving liquid/solid separation. For example, heavy liquids produced by indirect coal liquefaction have been separated from coal ash,[13] and mineral matter has been separated from shale oil.[14]

Experimental studies have been carried out by White and co-workers[15,16] to determine whether a catalyst-free wax (<0.1 wt %) can be produced from a slurry of F−T catalyst using NCE or supercritical extraction. A semicontinuous apparatus was used to process a slurry containing 5 wt % of an iron-based catalyst obtained from the AFDU. The solvents studied were *n*-butane, *n*-pentane, and *n*-hexane. Extraction temperatures and pressures ranged from 380 to 513 K and from 55 to 70 atm (5.6 to 7.1 MPa), respectively. In these studies, the extraction unit was followed by one or two recovery units where the wax was separated from the solvent by reducing the pressure. Wax containing <0.1 wt % catalyst was recovered using magnets external to the extraction unit. The extraction was also effective without magnets, but slightly more catalyst, 0.11 to 0.37 wt %, remained in the wax. The pressures in the first recovery unit ranged from about 3 to about 13 atm, probably too low for commercial operation because of the energy required for solvent recompression. Although these studies did not include the effect of the two recycle streams shown in Figure 1, the results are important in two respects: (1) they demonstrate the technical feasibility of producing a product that is essentially free of solid catalyst, and (2) they provide a starting point for the choice of solvent and operating conditions for the extraction step.

The critical issues of continuous process synthesis for NCE of F−T catalyst/wax slurries have not been con-

(7) Brown, D.; Bhatt, B.; Heydorn, E.; Stiegel, G.; Mahagaokar, U.; Hoek, A. *Further Development of the Slurry Phase Fischer−Tropsch Process at La Porte, Texas*; American Institute of Chemical Engineers 1997 Spring National Meeting, March 9−13, 1997, Houston, TX; Paper 27e.

(8) Chang, M.; Coulaloglou, C.; Matula, J. *Exxon's Natural Gas to Liquids Conversion Technology − AGC-21 Process*, American Institute of Chemical Engineers 1997 Spring National Meeting, March 9−13, 1997, Houston, TX; Paper 27b.

(9) Zhou, P. Z. *Status Review of Fischer−Tropsch Slurry Reactor Catalyst/Wax Separation Techniques*; prepared for U.S. DOE Pittsburgh Energy Technology Center, February 1991, Burns and Roe Services Corp., Contract Number DE-AC22−98PC88400, Subtask 43.02.

(10) Biales, J.; Sherrard, D.; Kilpatrick, P.; Roberts, G. *A New Approach to Catalyst Recovery and Recycling in Slurry Bubble Column Fischer−Tropsch Reactors*, American Institute of Chemical Engineers 1997 Spring National Meeting, March 9−13, 1997, Houston, TX; Paper 140a.

(11) McHugh, M.; Krukonis, V. *Supercritical Fluid Extraction Principals and Practice*; Butterworth Publishers: Stoneham, MA, 1986; pp 1−11.

(12) Gearhart, J. A.; Garwin, L. *Oil Gas J.* **1976**, *74*, 63−66.

(13) Adams, R. M.; Knebel, A. H.; Rhodes, D. E. *Chem. Engr. Prog.* **1979**, *75*, 44.

(14) Stutzer, D.; Brunner, G.; Peter, S. In *Chemical Engineering at Supercritical Fluid Conditions*; Paulaitis, M. E., Penninger, J. M. L., Gray, R. D., Jr., Davidson, P., Eds.; Ann Arbor Science, 1983; Chapter 21, pp 435−443.

(15) White, C. M.; Jensen, K. L.; Rohar, P. C.; Tamilia, J. P.; Shaw, L. J.; Hickey, R. F. *Energy Fuels* **1996**, *10*, 1067−1073.

(16) White, C. M.; Jensen, K. L.; Rohar, P. C.; Tamilia, J.; Shaw, L. J.; Hickey, R. F. *Separation of Fischer−Tropsch Catalyst/Wax Mixtures Using Dense-Gas and Liquid Extraction*; 8th International Conference on Coal Science, 1995; Elsevier Science B. V.: Oviedo, Spain.

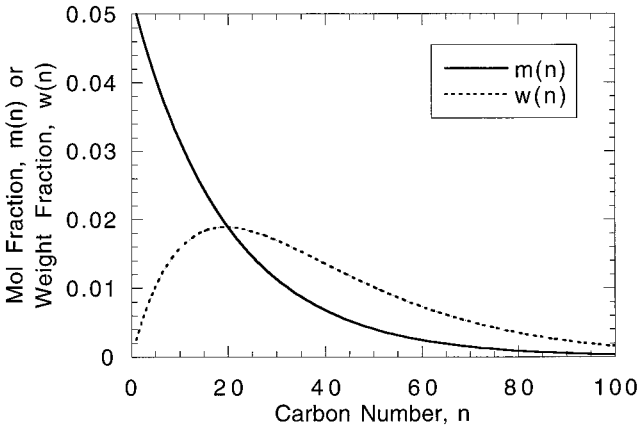

Figure 2. Anderson−Schulz−Flory product distributions for $\alpha = 0.95$.

sidered in detail. These issues include the choice of solvent, the solvent/slurry ratio, the ratio of slurry flowrate to the rate of hydrocarbon production, the buildup of light components in the solvent recycle loop, the buildup of heavy components in the reactor, and the conditions at which to operate the extraction and recovery units. The objective of this work was to evaluate the potential of the NCE process shown in Figure 1 by carrying out steady-state process simulations. This study was preliminary in nature. It was not intended to produce an optimized process design. In fact, one finding of this research is that the existing database of physical properties and vapor/liquid equilibrium models is not sufficient to support an optimum, or even reliable, process design. Rather, the intent of these simulations was to assess the basic technical feasibility of the NCE process concept and to define the technical issues that require additional study.

Scope

Although the F−T synthesis creates a range of products including paraffins, olefins, and some alcohols, only *n*-paraffins were considered in this research. A basis of 1000 kmol/h of product with an Anderson−Schulz−Flory (ASF) distribution of carbon numbers was used. The ASF distribution is characterized by a parameter α, the probability of chain growth, which is defined as the rate of chain propagation divided by the sum of the rates of propagation and chain termination. A value of $\alpha = 0.95$ was used for all of the simulations. This value is reasonably typical of the catalysts that might be used to produce a synthetic crude oil.

The ASF distribution is given by eq 1.[17]

$$m(n) = (1 - \alpha)\alpha^{(n-1)} \quad (1)$$

where n is the number of carbons in the product molecule and $m(n)$ is the mol fraction of the product that contains n carbons. The weight fraction, $w(n)$, is given by

$$w(n) = (1 - \alpha)^2 n\alpha^{(n-1)} \quad (2)$$

Both distributions are shown in Figure 2 for $\alpha = 0.95$. The cumulative weight percent between $n = 1$ and $n = 100$ is approximately 96.4%, i.e., about 3.6 wt % of the hydrocarbon product has a carbon number of 101 and higher when $\alpha = 0.95$. The cumulative mol percent up to and including $n = 100$ is 99.4%.

Simulations of the process of Figure 1 were run with *n*-pentane, *n*-hexane, *n*-heptane, and *n*-octane as solvents. Solvent imports would be virtually impossible if a F−T plant were located in a remote area. Therefore, the only species considered as solvents were products of the F−T synthesis. All simulations included one extraction unit and one or more recovery units. Unconverted H_2 and CO were not considered in the simulations, nor was the water and/or CO_2 produced by the reaction. The effect of these components is the subject of an ongoing study. Converged material balances were calculated for each process unit. Energy balances were not calculated.

Experimental Section

Flowsheet Simulation. The Aspen Plus simulation package was used to perform all calculations. The process was modeled by a series of MIXING and FLASH2 modules, as shown in Figure 3. MIXING modules were used to calculate mass balances when two or more inlet streams combined to give one outlet stream. FLASH2 units were used to calculate the vapor−liquid equilibria (VLE) for one inlet stream that separated into vapor and liquid outlet streams. The total pressure and temperature of all FLASH2 units were specified.

A MIXING unit (reactor Mixing unit) and FLASH2 unit (reactor Flash2 unit) were used to model the slurry reactor. Individual C_1 through C_{100} *n*-paraffins, with an ASF product distribution corresponding to $\alpha = 0.95$ (stream **1**), were fed continuously at a total rate of 1000 kmol/h to the reactor Mixing unit, where they combined with the recycled slurry (stream **6**) from the extraction unit. The combined inlet stream from the reactor Mixing unit (**2**) was divided into a vapor (**3**) and liquid product (**4**) using the reactor Flash2 unit. A temperature of 493 K and a total pressure of 10 atm were specified for the reactor Flash2 unit. These conditions are reasonably typical of those at which SBC F−T reactors operate, although this total pressure may be at the lower end of the preferred range.[3]

The extraction unit was also modeled with a MIXING module (SCE Mixing unit) and a FLASH2 module (SCE Flash2 unit). The liquid product from the reactor Flash2 unit (**4**) and a recycle stream (**11**) were combined in the SCE Mixing unit. The effluent from this unit (**5**) was separated into a light vapor phase (**7**) and a heavy phase (**6**) in the SCE Flash2 unit. The heavy stream (**6**) represented a slurry of the unextracted product and the solid catalyst, although the solid catalyst was not considered in these calculations. The presence of a solid affects the energy balance for the process and the viscosity of the slurry streams. However, there is no impact on the vapor/liquid equilibrium. The light stream (**7**) from the SCE Flash2 unit was sent to the recovery unit section.

The recovery unit was modeled by a FLASH2 unit (recovery Flash2 unit 1). In this unit, the temperature and/or pressure were chosen to condense the heaviest products (**8**). Uncondensed light components from the recovery Flash2 unit 1 (**9**) were recycled to the extraction unit via the recycle Mixing unit.

Additional recovery units were included in some runs. In this case, the condensed product (**8**) from the first recovery Flash2 unit was sent to a second recovery Flash2 unit, where additional solvent was vaporized and recycled to the recycle Mixing unit. When a third stage of recovery was included, the condensed product from the second recovery Flash2 unit was sent to the third recovery Flash2 unit, and the solvent vaporized was again recycled to the recycle Mixing unit.

(17) Satterfield, C. N., *Heterogeneous Catalysis in Industrial Practice (2nd ed.*; McGraw-Hill: New York, 1991; p 437.

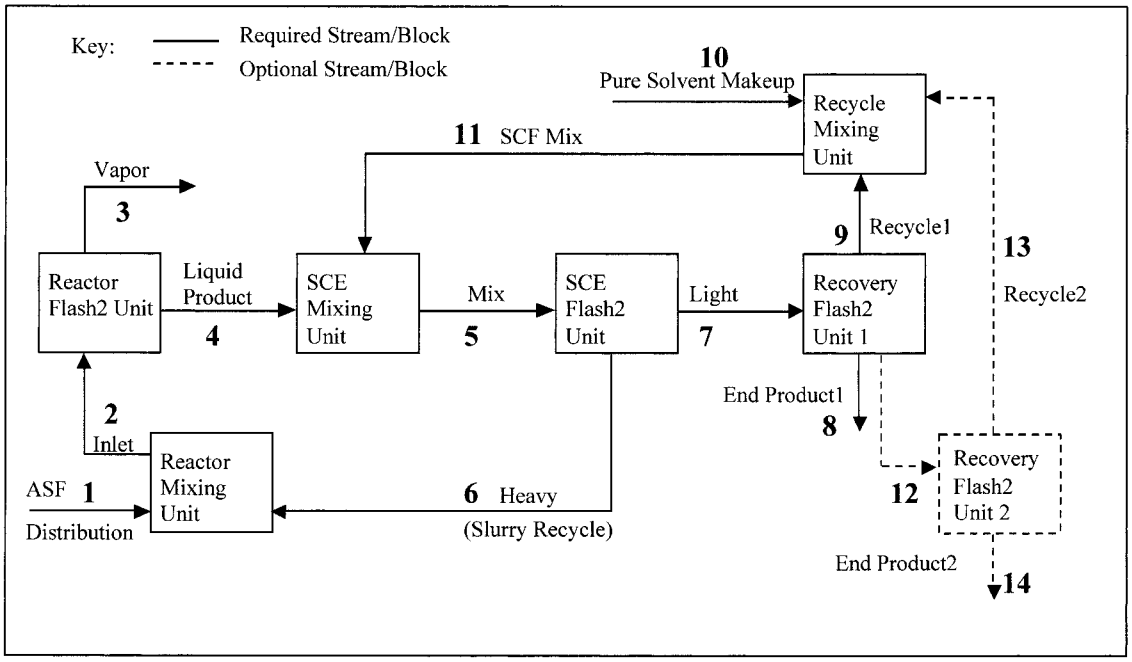

Figure 3. Process flowsheet showing ASPEN PLUS modules used for process simulation.

In all of the calculations, the solvent/nonsolvent molar ratio entering the extraction unit, i.e., in Stream **5**, was specified. The solvent/nonsolvent molar ratio was defined as

$$\text{ratio} = S/(T - S) \tag{3}$$

where S is the molar flowrate of the specified solvent in stream **5** and T is the total molar flowrate of stream **5**. There are computational advantages associated with specifying this ratio as an input parameter, and this definition has the benefit of including both the solvent in the slurry leaving the reactor and the solvent in the recycle stream (**11**) in S. A disadvantage of this definition is that the specific composition of the nonsolvent and the source of the nonsolvent are not considered. The nonsolvent ($T-S$) includes all compounds, ranging from C_1 to C_{100}, except for the designated solvent. Moreover, these compounds may enter stream **5** from the reactor (stream **4**) or from the light, recycle plus makeup, stream (**11**). Because the composition of the nonsolvent depends on the operating conditions of the extraction and recovery units, the solvent/nonsolvent ratio generally is not a reliable indicator of overall solvency. In fact, some of the "non-solvent" components are similar in carbon number to the "solvent" and contribute to the extraction of heavy components.

Stream Convergence. The steady-state mass balances were calculated using a sequential modular approach. This approach involves solving each of the Aspen modules in sequence, instead of solving a series of simultaneous algebraic equations. Exit stream results from the previous block are used as inlet compositions for the current block, and outlet compositions from the current block are used as inlet compositions for the following block. Since two recycle streams were involved, a set of initial estimates was required to begin the simulation. Estimates were made for all components in stream **5**, a tear stream, in Figure 3. Calculations then proceeded sequentially around both recycle loops.

New component values for the tear stream (**5**) were calculated for the last block in the sequence (SCE Mixing unit). If the new and old tear stream values *for each component* were within the convergence criterion shown in eq 4, the simulation was considered converged.

$$-0.0001 \le \frac{X_{\text{new}} - X_{\text{old}}}{X_{\text{old}}} \le 0.0001 \tag{4}$$

In the above, X_{old} is the previous value of the stream variable and X_{new} is the new value. When this criterion was not satisfied, new estimates were generated using the Wegstein method.[18]

For many cases, the component material balances were satisfactory when the convergence criterion of eq 4 was satisfied. However, in some cases, there was some error in the overall balances for the heaviest components. When this occurred, the material balance closure for each component could be brought within acceptable limits (<1%) by increasing the convergence criterion of eq 4 to $\pm 10^{-5}$. It should be noted that each component from C_1 through C_{100} was considered individually. There was no need to lump various ranges of *n*-paraffins together into psuedo-components.

As noted above, the solvent/nonsolvent molar ratio in the extraction unit, defined in eq 3, was used as a design specification. The ratio was maintained within a relative convergence criterion of 10^{-4} by varying the rate of solvent makeup (stream **10**) for each iteration. If the ratio was outside the tolerance on any iteration, a new estimate of the makeup flowrate was generated using the Secant method.[18]

The results of the process calculations were evaluated by examining five parameters:

(1) Makeup, the solvent makeup flowrate (stream **10**);

(2) (V/P), the ratio of the vapor flowrate entering the extraction unit (stream **11**) to the total production rate(ASF distribution, stream **1**);

(3) (L/P), the ratio of the slurry flowrate (stream **4**) entering the extraction unit to the total production rate (stream **1**);

(4) (E_s/ASF_s), the ratio of solvent in the End Product (e.g., solvent in stream **8**) to solvent produced in the reactor (solvent in the ASF Distribution, stream **1**); and

(5) average molecular weight (AMW) of the slurry in the reactor (stream **4**).

The *net* solvent requirement is a critical element of process feasibility. At steady state, the amount of solvent produced in the reactor (i.e., the solvent in stream **1**) plus the makeup (stream **10**) is equal to the amount of solvent in the vapor stream leaving the reactor (**3**) plus the amount in the end product stream (e.g., **8**). The solvent in the vapor stream is

(18) Aspen Technology Inc. *Aspen Plus User Guide, Vol. 2, Release 9.2*; Aspen Technology Inc.: Cambridge, MA, November, 1995; pp 10-1−10-17.

potentially recoverable. However, the solvent in the end product leaves the plant as an export. Ideally, the solvent in the end product should be less than the solvent produced in the reactor, i.e., the solvent component of stream (**1**). This would ensure that the amount of solvent in stream **3** is greater than the amount of makeup, stream **10**. The parameter E_s/ASF_s is the ratio of solvent in the end product (e.g., **8**) to solvent produced in the reactor. If the solvent flowrate in the end product (E_s) is less than the rate of solvent production (ASF_s), then E_s/ASF_s is less than 1. For this condition, no *net* import of solvent is required, assuming that all of the solvent in the vapor (**3**) is recovered.

High makeup flowrates indicate loss of solvent either in the vapor leaving the reactor (stream **3**) or in the end product (e.g., stream **8**). If the extraction conditions are such that large quantities of solvent are dissolved in the slurry recycle (stream **6**), there will be a large quantity of solvent in stream **3**. This is detrimental, as recovery of this solvent would lead to a high energy requirement for separation and recompression. The amount of solvent in stream **8** is determined primarily by conditions in the recovery unit.

The ratio *V*/*P* is defined as the total molar flowrate of the vapor stream entering the extraction unit (**11**) divided by the production rate (1000 kmol/h). It is a rough proxy for the size of the extraction and recovery units, and for the energy required for solvent recovery, recycle, and recompression. High *V*/*P* ratios are undesirable.

The ratio *L*/*P* is defined as the total molar flowrate of the liquid slurry leaving the Reactor (**4**) divided by the production rate (1000 kmol/h). This ratio indicates how much slurry must be fed to the extraction unit in order to recover all of the product. High *L*/*P* values are undesirable since they suggest the need for a larger slurry pump, and more heat exchange area between the reactor and the extraction unit.

A final consideration in evaluating process flowsheets was the average molecular weight (AMW) of the reactor slurry, i.e., that of stream **4**. A high AMW indicates a substantial recycle of heavy components back to the reactor, relative to recycle of lighter products, and suggests selective extraction of lighter products. If the AMW of the reactor slurry is too high, the resulting high viscosity of the slurry could cause undesirable effects in the reactor, i.e., low gas holdup, an unpumpable slurry, or mixture gelation. Several correlations exist relating the carbon number and temperature to the viscosity.[19]

Thermodynamics. All VLE calculations were performed with the Redlich−Kwong−Soave (RKS) equation of state, as shown in eq 5 below:

$$P = \frac{RT}{V_m - b} - \frac{a}{V_m(V_m + b)} \tag{5}$$

where:

$$a = \sum_i \sum_j x_i x_j (a_i a_j)^{0.5}(1 - K_{ij}) \tag{5a}$$

$$b = \sum_i x_i b_i \tag{5b}$$

$$a_i = (0.42747)\alpha_i \frac{R^2 T_{ci}^2}{P_{ci}} \tag{5c}$$

$$b_i = (0.08664)\frac{RT_{ci}}{P_{ci}} \tag{5d}$$

$$\alpha_i(T) = [1 + m_i(1 - T_{ri}^{0.5})]^2 \tag{5e}$$

$$m_i = 0.48 + 1.57\omega_i - 0.176\omega_i^2 \tag{5f}$$

$$\omega_i = -\log_{10}\frac{P_i(T_{ri} = 0.7)}{P_{ci}} - 1 \tag{5g}$$

$$T_{ri} = \frac{T}{T_{ci}} \tag{5h}$$

In eq 5, P is the absolute pressure, T is the absolute temperature, R is the gas constant, x is the mole fraction, ω is the acentric factor, T_r is the reduced temperature, T_c and P_c are the critical temperature and pressure, respectively, and K_{ij} is the binary interaction parameter. The subscripts *i* and *j* refer to chemical components. All simulations were performed with $K_{ij} = 0$. This was necessary because the data and/or correlations required for a more sophisticated approach are not available.

To use the RKS equation of state, values of T_c, P_c, and ω are needed for each compound. However, experimental values of T_c and P_c are not available for the *n*-paraffins above C_{24}. The values of T_c and P_c were estimated when experimental data was not available. From the values of T_c and P_c, and the Antoine constants[20] for the compound in question, ω was calculated on the basis of its definition in eq 5g.

Three correlations are available for estimating the critical constants. Two are based on Tsonopoulos and Tan's[21] modification of Flory theory. These authors fitted their equations to two different sets of experimental critical-constant data. Each data set had the same values of T_c and P_c from C_1 to C_{18}. However, the values for the critical density were different from C_5 to C_{10}. Each data set yielded different estimated critical constants. The third correlation[22] is empirical.

To determine the best set of estimated pure component critical constants to use in this research, experimental binary data for the C_4−C_{60} *n*-paraffin system[23] were compared with calculated binary data, using the RKS equation of state with three different sets of estimated critical constants, one from each correlation. The *Pxy* diagram was calculated using a FLASH2 unit, and the experimental C_4−C_{60} data was compared to the calculation.[24] The C_4−C_{60} system was chosen because it was the only one for which experimental binary data are available for a light (C_4−C_{10}) *n*-alkane and a heavy (C_{30}^+) *n*-paraffin. This system is similar to that of a light solvent and a heavy, F−T wax component. In addition, C_{60} is well beyond the range of the experimental T_c, P_c data, so it provides a critical test of the extrapolative ability of each of the three correlations.

Phase Diagrams. Prior to beginning the process simulations, binary P_{xy} phase diagrams and constant composition *PT* phase diagrams were generated to aid in selecting conditions for the extraction and recovery units. For all phase diagrams, a FLASH2 module was used to calculate the VLE. Diagrams were produced for *n*-butane, *n*-pentane, *n*-hexane, *n*-heptane, and *n*-octane with the components *n*-C_{20} and *n*-C_{100}. From these *Pxy* diagrams, a *PT* projection of mixture critical points was created.

Constant composition *PT* phase diagrams were calculated to determine the presence and location of any retrograde regions. Diagrams were generated for various mixtures of either *n*-pentane, *n*-hexane, or *n*-heptane with the ASF

(19) Mehrotra, A. K.; Monnery, W. D.; Svrcek, W. Y. *Fluid Phase Equilib.* **1996**, *117*, 344−355.

(20) Stephenson, R. M.; Stanislaw, M. *Handbook of the Thermodynamics of Organic Compounds*; Elsevier Publishing: New York, 1987; pp 16−471.

(21) Tsonopoulos, C.; Tan, Z. *Fluid Phase Equilib.* **1993**, *83*, 127−128.

(22) Teja, A. S.; Lee, R. J.; Rosenthal, D.; Anselme, M. *Fluid Phase Equilib.* **1990**, *56*, 153−169.

(23) Nieuwoudt, I. The Fractionation of High Molecular Weight Alkane Mixtures with Supercritical Fluids, *High-Pressure Chemical Engineering*; Elsevier Science: New York, 1996; pp 283−290.

(24) Sherrard, D. M. Personal communication. 1997.

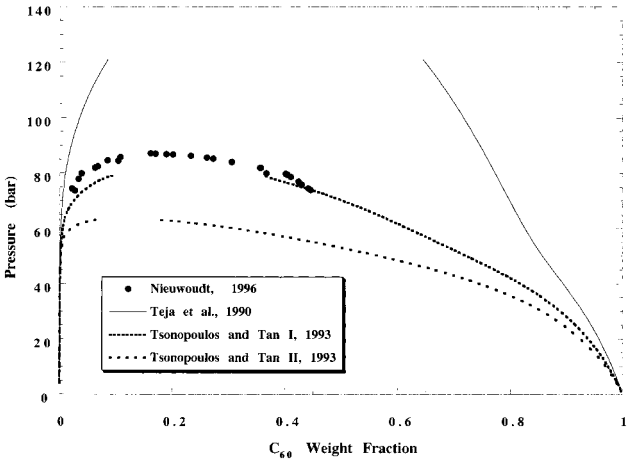

Figure 4. Comparison of experimental *Pxy* data for the C_4-C_{60} *n*-paraffin system with calculations based on the RKS equation of state with $K_{ij} = 0$ for three different sets of critical constants. $T = 453$ K.

distribution of *n*-alkanes from C_1 to C_{100} for $\alpha = 0.95$. This composition is not exactly the same as the composition of the stream entering the recovery unit because the effects of the two recycle loops are not included. Nevertheless, these diagrams proved useful in understanding the behavior of the recovery unit, at least on a semiquantitative basis. Solvent/nonsolvent molar ratios ranging from 3:1 to 20:1 were evaluated.

Results and Discussion

I. Phase Behavior. *Pure Component Critical Constants.* Experimental *Pxy* data for the C_4-C_{60} system at 453 K[23] are compared with calculations based on the RKS equation of state in Figure 4, for three different correlations of the pure component critical constants. The critical constants calculated using the Tsonopoulos and Tan correlation based on data set I[21] gave the closest match between the predicted and the experimental *Pxy* data. Therefore, critical constants calculated with that correlation were used in all of the process simulations described here. Numerical values of T_c and P_c can be found in Biales.[25]

Additional *Pxy* data for the C_4-C_{60} system are available at a lower temperature, 433 K.[23] The RKS equation of state with $K_{ij} = 0$ underpredicted the mixture critical pressure significantly at this temperature, for all three sets of critical constants. Therefore, the question of proper critical constants for high-carbon-number *n*-paraffins should not be considered resolved by the comparison shown in Figure 4.

Phase Behavior of F−T Products and Light n-Paraffins. The mixture critical points computed from the RKS equation of state for *n*-butane, *n*-pentane, *n*-hexane, *n*-heptane, and *n*-octane with C_{20} (eicosane) and C_{100} (hectane), respectively, are shown in Figures 5 and 6. As solvent size increases, the two-phase region for each binary moves to higher minimum temperatures and lower pressures for both solutes. In addition, the mixture critical curves become flatter, indicating a smaller two-phase region in *PT* space. All mixture loci are of Class I phase behavior.[27]

(25) Biales, J. M. Modeling and Evaluation of a Supercritical Extraction Process for Separating Fischer−Tropsch Wax from Catalyst. M.S. Thesis, North Carolina State University, 1997.

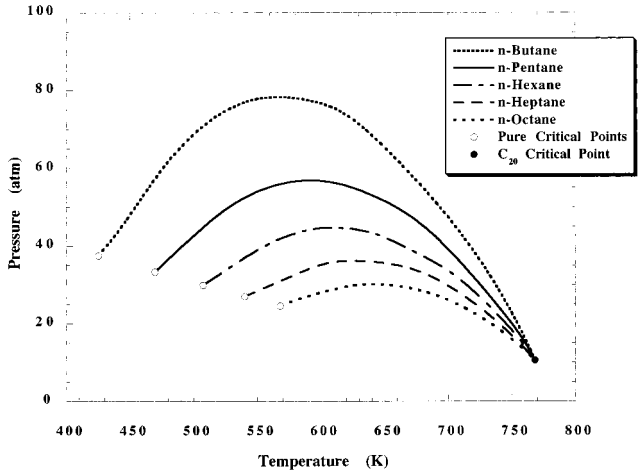

Figure 5. *PT* mixture critical curves for various solvents with eicosane (C_{20}). RKS equation of state, $K_{ij} = 0$

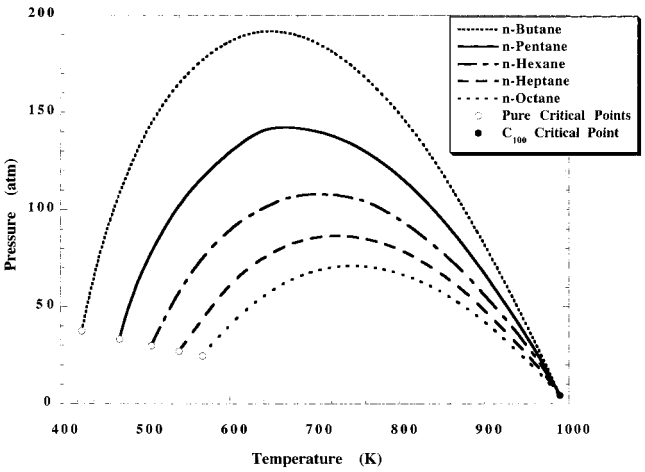

Figure 6. *PT* mixture critical curves for various solvents with hectane (C_{100}). RKS equation of state, $K_{ij} = 0$

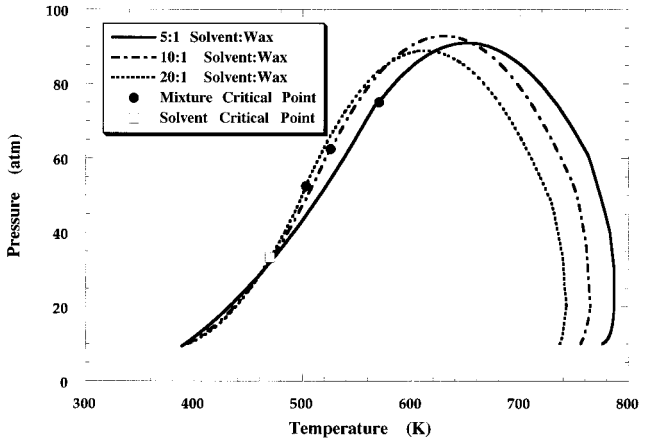

Figure 7. Constant composition *PT* diagram for *n*-pentane and ASF ($\alpha = 0.95$) mixture at various solvent:nonsolvent molar ratios. RKS equation of state, $K_{ij} = 0$

Figure 7 shows a constant-composition *PT* phase diagram for a product composition defined by the ASF ($\alpha = 0.95$) distribution. The solvent is *n*-pentane, and solvent/product ratios of 5, 10, and 20 are presented. As expected, the mixture critical point moves toward

(26) Brule, M. R.; Corbett, R. W. *Hydrocarbon Process.* **1984**, *63*, 73−77.

(27) Van Konynenburg, P. H.; Scott, R. L. *Philos. Trans. R. Soc.* **1980**, *298*, 495−540.

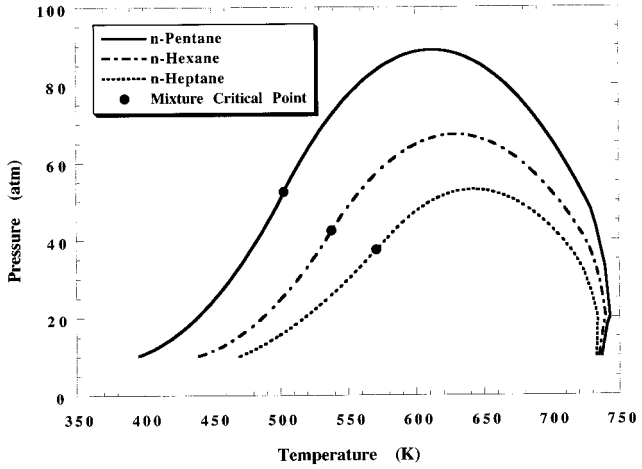

Figure 8. *PT* diagrams for ASF ($\alpha = 0.95$) mixture with various solvents at 20:1 solvent/nonsolvent molar ratio. RKS equation of state, $K_{ij} = 0$

the solvent critical point as the solvent/product ratio increases. All three curves have a retrograde region and a two-phase pressure maximum in the dew-point line. Similar results were observed for *n*-hexane and *n*-heptane.

Figure 8 shows constant-composition *PT* curves for three solvents at a solvent/product ratio of 20. As solvent size increases, both the mixture critical point and the maximum in the dew point line move to higher temperatures and lower pressures.

Taken collectively, these four figures offer some useful perspectives concerning the process of Figure 1. First, as the solvent size increases, the size of the region in which the process can be operated, i.e., the region of pressure and temperature in which two phases can exist, decreases, and the center of the region shifts to lower pressures and higher temperatures. Second, as the mixture being extracted becomes heavier, the region of operability expands and its center shifts toward higher temperatures and pressures. Finally, for a given solvent, the region of operability contracts and shifts to higher pressures and temperatures as the solvent/product ratio decreases.

Retrograde Condensation. A retrograde condensation region is a portion of the two-phase region where vapor quality is increased by raising pressure or dropping temperature. This is opposite to normal vapor−liquid equilibrium behavior. Retrograde regions may occur when a complex mixture of hydrocarbons contains large amounts of a light solvent. Brule and Corbett[26] explain this phenomena in terms of the topology of classes of phase diagrams. Six classes of binary VLE phase diagrams exist[27], although classes I and IV are more commonly found in hydrocarbon systems.[28]

Figure 9 shows a constant-composition *PT* phase diagram for a 20/1 molar ratio of *n*-pentane to F−T product, consisting of *n*-alkanes from C_1 to C_{100} corresponding to $\alpha = 0.95$. The mixture critical point lies close to the solvent critical point because the mixture contains such a large quantity of solvent. In addition, the two-phase pressure maximum lies on the dew point curve.

(28) Radosz, M. *Ind. Eng. Chem. Res.* **1987**, *26*, 2134−2139.

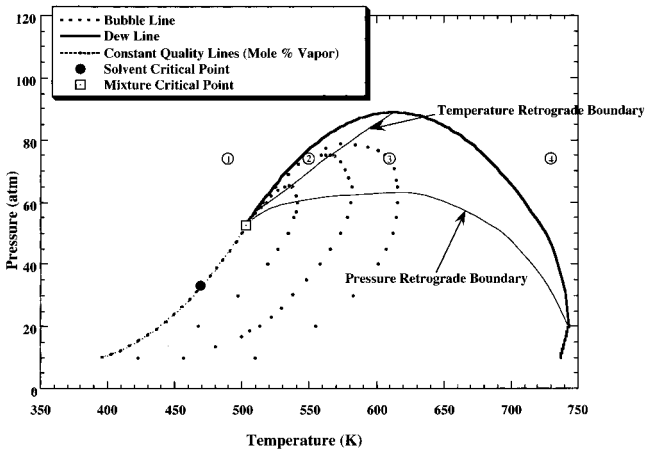

Figure 9. Constant composition *PT* diagram showing the retrograde region for a mixture containing *n*-pentane solvent and F−T product in a 20:1 molar ratio. RKS equation of state with $K_{ij} = 0$. The Fischer−Tropsch products are *n*-paraffins ranging from C_1 to C_{100}, with $\alpha = 0.95$.

Although the overall mixture composition is constant throughout the two-phase region, the fractions of vapor and liquid vary. Figure 9 shows three contours of constant molar vapor fraction. As usual, the dew point curve is 100% vapor and the bubble curve is 100% liquid. The locus of the pressure maxima for the curves of constant molar vapor fraction forms the boundary of the temperature-retrograde region.[26] Moving from point 1 to point 4 in Figure 9 illustrates the phase behavior associated with the temperature-retrograde region. At point 1, the temperature and pressure are such that the system is one phase, with a density and viscosity intermediate between liquid and vapor. As temperature is increased isobarically, the system enters the two-phase region by crossing the dew line and entering the retrograde region (point 2). At this point, the mixture is about 95 mol % vapor and 5 mol % liquid. Within the temperature-retrograde region, an increase in temperature causes additional liquid to condense, i.e., moves point 2 to a curve with a lower percent vapor. As the mixture is heated further from point 2 to point 3, the retrograde boundary is crossed and typical VLE behavior is observed, i.e., increasing temperature causes vaporization. Continuing from point 3 to point 4, the dew line is crossed again and the mixture is completely vaporized.

Product recovery through isobaric heating is of special interest because recompression of the recycled solvent vapor (**9**) can be eliminated or minimized. However, Figure 9 raises some question about the feasibility of employing temperature-retrograde condensation for product recovery. First, the temperature-retrograde region is narrow with respect to temperature, with a maximum width of about 25 K. Second, unless the pressure is very close to the mixture critical point, the extent of condensation is very limited. Those features suggest that a large solvent recycle stream and a high *V*/*P* ratio will be required in temperature-retrograde operation.

A region of pressure-retrograde behavior is also shown in Figure 9. At pressures above the lower boundary of this region, decreasing the pressure causes liquid to condense and increasing the pressure causes vaporiza-

Table 1. Effect of Recovery Temperature on Process Performance for Designs Incorporating Temperature-Retrograde Product Recovery[a]

extraction conditions		recovery conditions		calculated process parameters				
P_{ext} (atm)	T_{ext} (K)	P_{rec} (atm)	T_{rec} (K)	makeup (kmol/h)	AMW	*L*/*P*	*V*/*P*	E_s/ASF$_s$
60	520	60	525	207 000	446	25.1	392	78
60	520	60	540	59 600	420	7.3	119	62
60	520	60	560	40 600	395	4.8	80	43
60	520	60	570	37 900	381	4.2	70	36
60	520	60	580	41 100	375	4.3	71	31

[a] Solvent: *n*-pentane; solvent/non-solvent ratio = 20.

tion. The pressure-retrograde region is substantially larger than the temperature-retrograde region, and the latter is included completely in the former. In fact, a substantial portion of the two-phase region above the mixture critical pressure is in the pressure-retrograde region.

Finally, it should be emphasized that care must be exercized in applying the results of Figures 5−9 to actual process analysis. Both the light stream and the heavy stream that are contacted in the extraction unit of Figure 1 can be quite different in composition from the streams that formed the bases for Figures 5−9. The solvent recycle (**11**) will contain components that are both lighter and heavier than the designated solvent. Compounds that are lighter than the solvent will build up in the solvent recycle loop because any of these compounds that enter the separation system in Stream **4** can only leave the system by dissolving into the slurry recycle (**6**) or the end product (e.g., **8**), which will require a high partial pressure. Furthermore, the heavy stream (**4**) can contain high-carbon-number components that have built up to relative concentrations that are not represented accurately by the ASF distribution.

II. Process Simulations. The following results are intended to demonstrate the feasibility of designing a near-critical extraction process to recover the heavy product from a F−T slurry reactor. These results also illustrate the response of the process to changes in the important process variables. However, as stated in the Introduction, it was not an object of this work to identify an optimum process design.

Temperature-Retrograde Condensation Simulations. For this group of process simulations, condensation in the recovery unit was achieved by isobarically raising the temperature of the light stream (**7**) leaving the extraction unit. For *n*-pentane, *n*-hexane, and *n*-heptane, feasible designs based on temperature-retrograde condensation were developed at a 20:1 solvent/nonsolvent molar ratio for extraction and recovery pressures in the range of 50−60, 40−50, and 35−40 atm, respectively. Extraction temperatures varied between 515 and 530 K, 535 and 580 K, and 570 and 600 K for *n*-pentane, *n*-hexane, and *n*-heptane, respectively. These solvent/nonsolvent ratios are considerably lower than those used by White and co-workers,[15,16] and the present extraction pressures for *n*-pentane and *n*-hexane are lower while the extraction temperatures are 50 to 100 K higher. However, at least some of the extractions of White and co-workers appear to be at supercritical conditions, since essentially all of the hydrocarbon in the catalyst/wax slurry was extracted into the liquid phase.

Recovery Temperature. Table 1 compares process performance for five temperature-retrograde simulations with *n*-pentane, where only the recovery temperature was varied. As recovery temperature increased from 525 K, the makeup, *V*/*P* ratio, and *L*/*P* ratio decreased and went through minima at about 570 K. However, the increase in makeup between 570 and 580 K suggests that the latter temperature may be somewhat outside the region in which temperature-retrograde condensation occurs. The range of temperatures in Table 1 is wider than suggested by Figure 9. The AMW and E_s/ASF$_s$ ratio decreased with increasing recovery temperature, but did not go through minima. Since ASF$_s$ is 40.7 kmol/h for *n*-pentane, the values of E_s/AFS$_s$ show that the majority of the makeup requirement results from dissolution of the solvent into the liquid stream that is recycled to the reactor, followed by vaporization from the reactor.

Solvent Comparison. Three solvents (*n*-pentane, *n*-hexane, and *n*-heptane) are compared in Table 2 under conditions where temperature-retrograde condensation was used for product recovery. This table shows the process parameters for the designs with the lowest required makeup, for each solvent. These designs resulted from a coarse exploration of the process design variables; they are not the result of a rigorous optimization. The operating region for *n*-pentane, i.e., the pressure and temperatures of the extraction and recovery units, approximates the temperature retrograde region shown in Figure 9, although, as noted previously, the difference between the extraction and recovery temperatures, about 50 K, is considerably greater than the width of the retrograde condensation region in Figure 9. This may be the result of the broader range of compounds that are present in the light phase entering the recovery unit and the different composition of the heavy product in the converged process simulation.

The difference in temperature between the extraction and recovery units was smaller for *n*-hexane and *n*-heptane than for *n*-pentane, 27 and 10 K, respectively, compared to 50 K for *n*-pentane. This suggests that the temperature-retrograde regions for the heavier solvents were narrower, at least at a 20:1 solvent/nonsolvent ratio.

The AMW of the reactor contents for *n*-heptane (222) is substantially lower than the average molecular weight of the ASF products (278). Therefore, the viscos-

Table 2. Parameters for Process Designs Incorporating Temperature-Retrograde Product Recovery[a]

	extraction conditions		recovery conditions		calculated process parameters				
solvent	P_{ext} (atm)	T_{ext} (K)	P_{rec} (atm)	T_{rec} (K)	makeup (kmol/h)	AMW	*L*/*P*	*V*/*P*	E_s/ASF$_s$
n-pentane	60	520	60	570	37 900	381	4	70	36
n-hexane	50	570	50	597	60 700	316	14	228	41
n-heptane	40	590	40	600	68 600	222	27	228	73

[a] The design with the lowest makeup for each solvent is shown; solvent/non-solvent ratio = 20.

Table 3. Effect of Extraction Temperature on Process Performance for Designs Incorporating Pressure-Retrograde Product Recovery[a]

extraction conditions		recovery conditions		calculated process parameters				
P_{ext} (atm)	T_{ext} (K)	P_{rec} (atm)	T_{rec} (K)	makeup (kmol/h)	AMW	*L*/*P*	*V*/*P*	E_s/ASF_s
60	515	40	515	46 600	509	6.5	96	40
60	525	40	525	70 200	590	15.3	233	30
60	540	40	540	90 100	612	29.0	453	22
60	550	40	550	86 100	603	33.6	541	19
60	560	40	560	72 200	584	33.2	563	17
60	580	40	580	34 400	524	20.7	456	15

[a] Solvent: *n*-pentane; solvent/non-solvent ratio = 20.

Table 4. Effect of Recovery Pressure on Process Performance for Designs Incorporating Pressure-Retrograde Product Recovery[a]

extraction conditions		recovery conditions		calculated process parameters				
P_{ext} (atm)	T_{ext} (K)	P_{rec} (atm)	T_{rec} (K)	makeup (kmol/h)	AMW	*L*/*P*	*V*/*P*	E_s/ASF_s
50	570	36	570	no separation (overextraction)				
50	570	37	570	13 900	355	4.9	95	43
50	570	40	570	16 400	352	5.4	99	49
50	570	43	570	20 700	345	6.2	110	60
50	570	45	570	28 500	343	8.1	134	66

[a] Solvent: *n*-hexane; solvent/non-solvent ratio = 20.

ity of the liquid in the reactor for these cases should be lower than it would be if filtration were used for product recovery. With filtration, the AMW of the liquid exceeds the average molecular weight of the ASF distribution because the lightest components of the ASF distribution are essentially completely vaporized at reactor conditions.

Pressure-Retrograde Condensation Simulations. For this portion of the study, product was recovered by reducing the pressure isothermally, i.e., the extraction and recovery unit temperatures were the same. Various extraction temperatures and pressures were studied using *n*-pentane, *n*-hexane, and *n*-heptane as solvents. Solvent/nonsolvent molar ratios were 20:1 for all three solvents.

Temperature. Some typical results for pressure-retrograde condensation simulations with *n*-pentane are shown in Table 3. The extraction/recovery temperature varied between 515 and 580 K, at otherwise constant conditions. This table shows that the makeup and the AMW went through maxima at 540 K. Figure 9 shows that the lower boundary of the pressure-retrograde region also goes through a maximum with increasing temperature. The maxima in the makeup flow rate and the AMW may be the result of a recovery pressure that is below this lower boundary, especially at intermediate temperatures. However, care must be taken in using Figure 9 to interpret the results in Table 3, since the compositions of both the "solvent" and the "product" are different in the process simulations and in Figure 9.

Recovery Pressure. The effect of recovery pressure was studied using *n*-hexane as solvent. Table 4 shows that makeup, *L*/*P* ratio, *V*/*P* ratio, and E_s/ASF_s ratio all decreased with decreasing recovery pressure. In fact, the makeup at the lowest recovery pressure, 37 atm, is the lowest observed in any of the pressure-retrograde simulations. Below 37 atm, the simulation did not converge because there was no heavy phase leaving the extraction unit. This condition is referred to as "overextraction".

Comparison to Temperature-Retrograde Operation. In general, the makeups for the pressure-retrograde simulations were somewhat lower than those for the temperature-retrograde designs. However, the lowest *V*/*P* and *L*/*P* ratios are similar for the two modes of product recovery. Moreover, the major energy requirements associated with pressure-retrograde and temperature-retrograde operation are roughly comparable. For example, with the *n*-hexane design in Table 4 at $P_{rec} = 37$ atm, about 81 000 kmol/h of vapor must be recompressed by 13 atm. This is stream **9** in Figure 3, calculated as (*V*/*P* × 1000 − makeup). In addition, the makeup of about 14 000 kmol/h must be recompressed by about 40 atm, from the pressure of the reactor, 10 atm, to the pressure of the extraction unit, 50 atm. This assumes that about 1500 kmol/h of *n*-hexane, the "excess" solvent in the end product, over and above the amount corresponding to $E_s/ASF_s = 1$, will be recovered at 10 atm. In comparison, the temperature-retrograde run with *n*-hexane that had the lowest makeup (Table 2) would require heating about 170 000 kmol/h, calculated as (*V*/*P* × 1000 − makeup − 1000), by 27 K between the extraction and recovery units, and that the makeup of approximately 61 000 kmol/h be recompressed from approximately 10 atm to 50 atm. The total compression requirement for the temperature-retrograde design, 2.4×10^6 kmol atm h^{-1}, is comparable to that of the pressure-retrograde design, 1.6×10^6 kmol atm h^{-1}, considering that neither design is optimized.

The E_s/ASF_s ratios were substantially greater than 1 for all of the pressure- and temperature-retrograde simulations. Therefore, additional recovery units would be required for solvent self-sufficiency.

Low Solvent/Nonsolvent Ratio Simulations. Simulations also were performed at low solvent/nonsolvent molar ratios. Table 5 contains the parameters for the designs with the lowest makeups for each solvent: *n*-pentane, *n*-hexane, *n*-heptane, and *n*-octane. Product recovery was accomplished by a combination of pressure-retrograde condensation and temperature reduction. With all four solvents, the makeup flow rates are significantly lower than the makeups obtained in the retrograde-condensation regions, using higher solvent/

Table 5. Process Parameters for Low Solvent/Non-Solvent Ratio Runs with the Lowest Makeup Flow Rates

	extraction conditions			recovery conditions		calculated process parameters				
solvent	P_{ext} (atm)	T_{ext} (K)	ratio[a]	P_{rec} (atm)	T_{rec} (K)	makeup (kmol/h)	AMW	*L*/*P*	*V*/*P*	E_s/ASF_s
n-pentane	34	680	3.1	31	630	4 250	504	30	136	9.2
n-hexane	38	670	3.0	38	650	5 840	349	43	109	18
n-heptane	36	650	3.0	30	630	1 660	269	35	156	23
n-octane	40	650	3.35	30	630	1 750	199	12	34	41

[a] Solvent/non-solvent ratio.

Table 6. Effect of Extraction Pressure on Process Performance for Designs with Low Solvent/Non-Solvent Ratios[a]

extraction conditions		recovery conditions		calculated process parameters				
P_{ext} (atm)	T_{ext} (K)	P_{rec} (atm)	T_{rec} (K)	makeup (kmol/h)	AMW	*L*/*P*	*V*/*P*	E_s/ASF_s
35	650	30	630	no separation (overextraction)				
36	650	30	630	1 660	269	35	156	22
38	650	30	630	2 600	253	65	109	24
40	650	30	630	6 940	243	135	83	24
41	650	30	630	25 700	254	294	99	22
42	650	30	630	no separation (underextraction)				

[a] Solvent: *n*-heptane; solvent/non-solvent ratio = 3.

nonsolvent ratios. The makeup flow rates for these low solvent/nonsolvent designs range from about 1.7 to about 5.8 times the product basis. The makeups for the best retrograde-condensation runs were approximately 14 to 70 times the product basis. The AMW trended downward with increasing solvent size, and was less than the average molecular weight of the ASF distribution with *n*-heptane and *n*-octane. The E_s/ASF_s ratios increased with increasing solvent size, and were greater than 1 in all four cases.

Extraction Pressure. Table 6 shows the parameters for four *n*-heptane designs with extraction pressures ranging from 35 to 42 atm, with all other conditions constant. As extraction pressure was decreased, the makeup decreased. The AMW and the E_s/ASF_s ratio did not change significantly over the range of extraction pressure studied. Since ASF_s for *n*-heptane is about 37 kmol/h, approximately half of the required makeup for the design at 36 atm results from solvent in the product stream. The *V*/*P* ratio went through a flat minimum with extraction pressure, but the *L*/*P* ratio decreased significantly with decreasing pressure. The *V*/*L* ratios are very low for these runs, below 1 in some cases.

Feasibility. The results of the low solvent/nonsolvent simulations are interesting because of the low makeup flow rates that are required. The makeups were as low as 1.7 times the production rate, and a *V*/*P* ratio as low as 34 was achieved. The compression requirement for the *n*-hexane design in Table 5 is only about 1.6×10^5 kmol atm h^{-1}, roughly a factor of 10 lower than for the best runs at high solvent/nonsolvent ratios. A potential problem with the low solvent/nonsolvent region is the high operating temperatures of the extraction unit, 650−680 K, that appear to be required. These high temperatures might cause deactivation of the F−T catalyst.

Staged Recovery Units. Since an E_s/ASF_s ratio of less than one was not achieved with a single recovery unit, a few simulations were carried out with multiple recovery units to establish the feasibility of reducing the E_s/ASF_s ratio to less than one, and to explore the influence of multiple recovery units on overall system behavior. Table 7 shows the effect of adding additional recovery units in series, as shown in Figure 3, with the operating conditions of the extraction unit and the first recovery unit held constant. With a second recovery unit, operating at a marginally lower pressure than the first recovery unit (32 atm vs 34 atm), the E_s/ASF_s ratio decreased from 9.1 to 8.4, and the makeup flow rate decreased about 2.5%. Reducing the pressure in the second recovery unit to 20 atm changed the operation of the whole system, such that only a light phase left the extraction unit (overextraction).

To compensate, the solvent/nonsolvent ratio was reduced to 2, with the same operating conditions in the extraction and the two recovery units. The E_s/ASF_s ratio decreased to about 4, but the makeup increased by about a factor of 3. This increase was caused by increased dissolution of *n*-pentane into the liquid leaving the extraction unit. Reducing the pressure in the second recovery unit to 10 atm reduced the E_s/ASF_s ratio to about 1.7 and had very little effect on the makeup flow rate.

A third recovery unit then was added, operating at the same temperature as the first and second recovery units, but at a pressure of 5 atm. The E_s/ASF_s ratio was 0.7 for this design. This demonstrates that the E_s/ASF_s ratio can be reduced to less than one. However, the calculations in Table 7 also show that the operation of a system of recovery units can cause changes in the performance of the overall process, and require adjustment of the operating conditions. Further studies are required to understand how multiple recovery units are best utilized.

Conclusions

(1) The Aspen Plus process simulation program is a useful tool for analyzing the F−T NCE process. Converged material balances were obtained over a wide range of operating conditions. It was not necessary to utilize psuedo-components in order to obtain solutions in a reasonable computing time.

(2) The thermodynamic properties used in these calculations are not sufficiently accurate to support an optimum or reliable process design. Properties such as the critical temperature and pressure and the acentric factor need to be determined experimentally for heavy C_{30}^+ hydrocarbons to predict vapor/liquid equilibrium with a cubic equation of state such as RKS. A method for predicting binary interaction parameters also is required.

Table 7. Effect of Additional Product Recovery Units on Process Performance[a]

number of recovery units	recovery unit 1		recovery unit 2		recovery unit 3		solvent/ non-solvent ratio	solvent makeup	E_s/ASF_s
	T (K)	*P* (atm)	*T* (K)	*P* (atm)	*T* (K)	*P* (atm)			
1	650	34					3	8000	9.1
2	650	34	650	32			3	7800	8.4
2	650	34	650	20			3	no solution (overextraction)	
2	650	34	650	20			2	23500	4.0
2	650	34	650	10			2	22600	1.7
3	650	34	650	20	650	5	2	21800	0.7

[a] Extraction temperature = 680 K; pressure = 34 atm; solvent = *n*-pentane.

Changes in the thermodynamic parameters that were used in this study will change the calculated values of the makeup, *V*/*P*, AMW, etc., at a fixed set of operating conditions. However, there is no a priori reason to believe that the magnitude and/or direction of any required parameter adjustments would change the basic conclusion of this study, i.e., that NCE is a technically feasible approach to catalyst/wax separation.

(3) The best results in terms of lowest solvent makeup flow rates, lowest *V*/*P* ratios, and lowest E_s/ASF_s ratios were achieved at low solvent/nonsolvent ratios. However, the high extraction temperatures of 630−680 K that were associated with low solvent/nonsolvent ratios might cause catalyst deactivation. If experimental studies were to confirm this concern, operation at low solvent/nonsolvent ratios might not be technically feasible. However, the present results show that the temperature of the extraction unit can be reduced by using higher solvent/nonsolvent ratios and lighter solvents. There should be sufficient room to adjust the design and operation of the NCE process to solve any problem of catalyst deactivation that might result from high temperatures in the extraction unit.

(4) More than one recovery unit may be necessary to recover enough solvent to make the F−T plant self-sufficient. This should not be a major economic issue, since these vessels will operate at a lower pressure and should not require complex internals, and since additional recovery units beyond the first should not contribute significantly to the recompression requirement.

Acknowledgment. This research was supported under Department of Energy, Federal Energy Technology Center, University Coal Research Program Contract Number DE-FG22-94PC94219, via a sub-contract with Clemson University. The authors thank Professor Mark C. Thies of Clemson University for many helpful discussions. Special thanks are extended to Ms. Diane M. Sherrard for carrying out various thermodynamic analyses that provided a basis for this research, and to Ms. Elizabeth L. Dodge for conducting some of the process simulations.

EF980208U